

Supporting Information

Visible-Near-Infrared Absorbing A- π_2 -D- π_1 -D- π_2 -A Type Dimeric Porphyrin Donor for High Performance Organic Solar Cells

Song Chen,^{‡ a} Lei Yan,^{‡ b} Liangang Xiao,^{‡ c} Ke Gao,^c Wei Tang,^b Cheng Wang,^d Chenhui Zhu,^d Xingzhu Wang,^{b} Feng Liu,^{e*} Xiaobin Peng,^{c*} Wai-Kwok Wong,^a and Xunjin Zhu^{a*}*

^a Department of Chemistry and Institute of Advanced Materials, Hong Kong Baptist University, Waterloo Road, Kowloon Tong, Hong Kong, P. R. China.

E-mail: xjzhu@hkbu.edu.hk

^b College of Chemistry, Xiangtan University, Xiangtan, Hunan, 411105, P. R. China.

E-mail: xzawang@xtu.edu.cn

^c State Key Laboratory of Luminescent Materials and Devices, South China University of Technology, 381 Wushan Road, Guangzhou, 510640, P. R. China.

E-mail: chxbpeng@scut.edu.cn

^d Advanced Light Source, Lawrence Berkeley National Lab, Berkeley, CA, 94720, United State

^e Department of Physics and Astronomy, and Collaborative Innovation Center of IFSA (CICIFSA), Shanghai Jiaotong University, Shanghai, 200240, P. R. China.

E-mail: fengliu82@sjtu.edu.cn

Experimental Procedures

Characterization

¹H NMR spectra were recorded using a Bruker Ultrashield 400 Plus NMR spectrometer. High-resolution matrix-assisted laser desorption/ionization time-of-flight (MALDI-TOF) mass spectra were obtained with a Bruker Autoflex MALDI-TOF mass spectrometer. UV-Vis spectra of dilute solutions (1×10^{-5} M) of samples in dichloromethane (DCM) were recorded at room temperature (ca. 25°C) using a Shimadzu UV-3600 spectrophotometer. Solid films for UV-Vis spectroscopic analysis were obtained by spin-coating the molecule solutions onto a quartz substrate. Cyclic voltammetry (CV) of the molecule solution was performed using a Versastat II electrochemical workstation in a standard three-electrode configuration equipped with a silver wire pseudo-reference, platinum wire counter electrode and glassy carbon working electrode. The cyclic voltammetry experiments were performed in an anhydrous solution of dichloromethane (CH_2Cl_2) with ~ 0.1 M tetrabutylammoniumhexafluorophosphate (TBAPF_6) supporting electrolyte. The potentials were measured against an Ag/Ag^+ (0.01 M AgNO_3) reference electrode; the ferrocene/ferrocenium ion (Fc/Fc^+) pair was used as the external standard. Samples were scanned at a rate of 50 mV/s following a dry N_2 purge to deoxygenate the solution. The onset potentials were determined from the intersection of two tangents drawn at the rising and background currents of the cyclic voltammograms. Estimations of the energy levels were obtained by correlating the onset ($E_{\text{ox}} \text{Fc}/\text{Fc}^+$, $E_{\text{red}} \text{Fc}/\text{Fc}^+$) to the normal hydrogen electrode (NHE), assuming a IP energy of 4.80 eV for Fc/Fc^+ . Optical band gap estimated from the formula of $1240/\lambda_{\text{onset}}$, λ_{onset} is the absorption onset of the film spectrum. The IP and EA values were calculated by the the oxidation and reduction potentials in solution: $E_{\text{IP}} = E_{\text{ox}} + 4.8$ (eV), $E_{\text{EA}} = E_{\text{red}} + 4.8$ (eV). And HOMO and LUMO energies can be also given by the following equation: $E_{\text{HOMO}} = -(E_{\text{ox}} + 4.8)$ (eV), $E_{\text{LUMO}} = -(E_{\text{red}} + 4.8)$ (eV).

Device Fabrication

Solution-processed bulk-heterojunction solar cells were fabricated as follows: Indium tin oxide (ITO) coated glass substrates were cleaned prior to device fabrication by sonication in acetone, detergent, distilled water, and isopropyl alcohol. After treated with an oxygen plasma for 5 min, 40 nm thick poly(styrenesulfonate)-doped poly(3,4-ethylenedioxythiophene) (PEDOT:PSS) (Bayer Baytron 4083) layer was spin-coated on the ITO-coated glass substrates at 2500 rpm for 30s, the substrates were subsequently dried at 150°C for 10 min in air and then transferred to a N₂-glovebox. The active layers were spun from solution of donor material:PC₇₁BM at weight ratio of 4:5 (or other ratio) with an overall concentration of 20 mg/mL. The thicknesses of active layers were measured by a profilometer. Finally, Al (~80 nm) was evaporated with a shadow mask as the top electrode. The effective area was measured to be 16 mm². Hole mobilities of the blends were measured by the space charge limited current (SCLC) method using ITO/PEDOT:PSS/CS-DP:PC₇₁BM/MoO₃/Al device structure.

Device Characterization and Measurement

The values of power conversion efficiency were determined from *J-V* characteristics measured by a Keithley 2400 source-measurement unit under AM 1.5G spectrum from a solar simulator (Oriel model 91192). Masks made from laser beam cutting technology with a well-defined area of 16 mm² were attached to define the effective area for accurate measurement. Solar simulator illumination intensity was determined using a monocrystal silicon reference cell (Hamamatsu S1133, with KG-5 visible color filter) calibrated by the National Renewable Energy Laboratory (NREL). The active layer was spin coated from blend chloroform or chlorobenzene solutions with a weight ratio of donor materials and PC₇₁BM at 1:1 (or other ratios) and then was placed in a glass petri dish containing 0.3 mL THF for 15s for solvent vapor annealing. The atomic force microscopy (AFM) measurements of the surface morphology of blend films were conducted on a NanoScope NS3A system (Digital Instrument). External quantum efficiency (EQE) values of the encapsulated devices were measured by using an integrated system (Enlitech, Taiwan, China) and a lock-in amplifier with

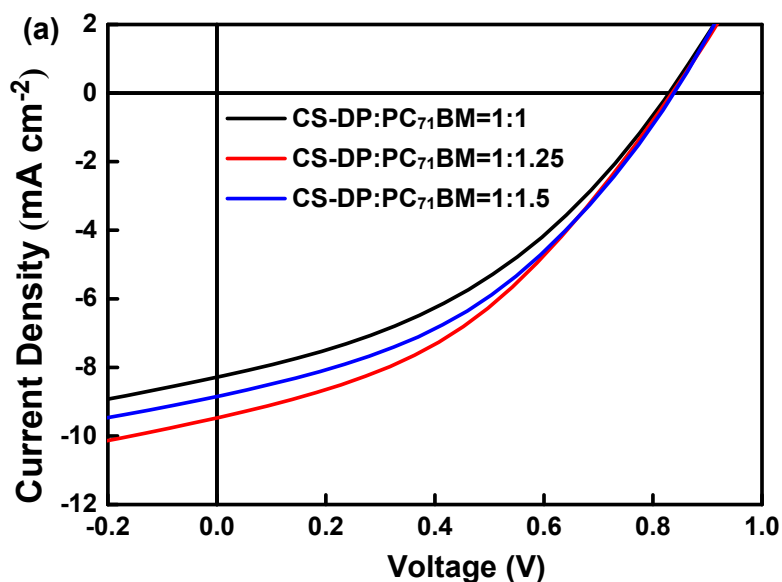
a current preamplifier under short-circuit conditions. The devices were illuminated by monochromatic light from a 100 W xenon lamp. The light intensity was determined by using a calibrated silicon photodiode.

Morphology Characterization

Grazing-incidence wide-angle X-ray scattering (GIWAXS) was done at either beamline 7.3.3 Lawrence Berkeley National Lab (LBNL). The sample was put inside a helium chamber, and Pilatus 2M detector was used to collect the signal. GIWAXS results were analyzed using Nika software package and peak information was accessed by gaussian fitting. RSoXS was performed at beamline 11.0.1.2 Lawrence Berkeley National Lab. Thin films was flowed and transferred S_{16} onto Si_3N_4 substrate and experiment was done in transition mode. AFM was performed on a Digital Instruments Dimension 3100, operating in tapping mode.

Device Optimization

Devices were optimized in the 1) donor:acceptor ratio; 2) solvent vapour annealing time.



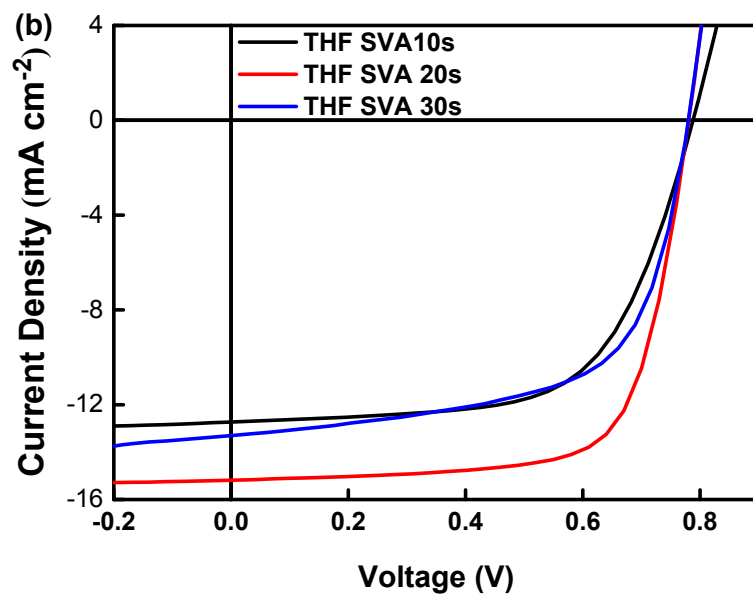


Figure S1. (a) Current density-voltage (J - V) curves of difference rate of **CS-DP**: PC_{71}BM devices; (b) Current density-voltage (J - V) curves of **CS-DP**: PC_{71}BM (4:5) with SVA devices.

Table S1. Photovoltaic performance of the solar cells based on **CS-DP**/ PC_{71}BM with different mixture rate under illumination of AM 1.5 G, 100 mW cm^{-2} .

Rate	Additive	Annealing °C	J_{sc} (mA cm^{-2})	V_{oc} (V)	FF (%)	PCE (best) (%)
1.0:1.0	3% Pyridine	90	8.30	0.828	39.8	2.73 ± 0.15 (2.89)
1.0:1.25	3% Pyridine	90	9.50	0.837	42.2	3.36 ± 0.23 (3.58)
1.0:1.5	3% Pyridine	90	8.89	0.840	43.3	3.22 ± 0.1 (3.32)

The average values are calculated from 16 devices with standard deviation.

Table S2. Photovoltaic performance of the solar cells based on **CS-DP/PC₇₁BM** with different THF vapor annealing time under illumination of AM 1.5 G, 100 mW cm⁻².

Treatment time (s)	Additive	Annealing °C	J_{SC} (mA cm ⁻²)	V_{OC} (V)	FF (%)	PCE (best) (%)
10	3% Pyridine	110	12.72	0.784	64.0	6.38±0.12(6.50)
20	3% Pyridine	110	15.14	0.781	69.8	8.23± 0.06(8.29)
30	3% Pyridine	110	13.30	0.780	63.1	6.55±0.32(6.87)

The average values are calculated from 16 devices with standard deviation.

Synthetic Route

Synthesis of compound 1

PZnBr₂ (1 g, 1.055 mmol) was mixed 4-ethynyl-2,5-bis(hexyloxy)benzaldehyde (313.3 mg, 0.950 mmol, ~0.9 eq) in 50 ml of THF and 20 ml of triethylamine. After degassed with N₂ for 20 min, Pd(PPh₃)₄ (60 mg, 0.053 mmol) and CuI (10 mg, 0.053 mmol) were added to the solution under an N₂ atmosphere. The reaction was stirred at 40°C for 24 hours. The completion of the reaction was monitored by TLC. The solvent was removed by rotary evaporation. The residue was purified by column chromatography using CH₂Cl₂/*n*-hexanes = 1/2 as eluent to give compound **1** (403 mg, 32%). ¹H NMR (400 MHz, CDCl₃) δ (ppm): 0.68–0.78 (m, 12H), 0.85–1.06 (m, 30H), 1.16–1.38 (m, 12H), 1.39–1.59 (m, 16H), 1.82 (m, 2H), 1.96 (m, 2H), 2.34 (m, 2H), 2.73 (m, 4H), 2.93 (m, 4H), 4.23 (m, 2H), 4.34 (m, 2H), 7.48 (s, 2H), 9.59–9.71 (m, 6H), 9.87 (m, 2H), 10.46 (s, 1H).

Synthesis of compound 2

Compound **1** (200 mg, 0.166 mmol), Pd(PPh₃)₄ (22 mg, 0.019 mmol), CuI (4 mg, 0.021 mmol) were mixed in THF (20 mL) and triethylamine (5 mL) to yield a green solution under nitrogen atmosphere. A solution of (triisopropylsilyl)acetylene (75 mg, 0.412 mmol) in triethylamine (5 mL) was slowly added to the reaction mixture at room temperature. The reaction mixture was then stirred at 40°C for overnight to give

deep green suspension. The completion of the reaction was verified by spot TLC. The solvent was then removed under reduced pressure, and the residue was chromatographed on silica gel using *n*-hexane as eluent to give compound **2** (156 mg, 72%). ¹H NMR (400 MHz, CDCl₃) δ (ppm): 0.67–0.75 (m, 12H), 0.85–1.32 (m, 47H), 1.39–1.61 (m, 32H), 1.84 (m, 2H), 1.96 (m, 2H), 2.35 (m, 2H), 2.68 (m, 4H), 2.91 (m, 4H), 4.28 (t, *J* = 6.4 Hz, 2H), 4.38 (t, *J* = 6.4 Hz, 2H), 7.52 (s, 1H), 7.55 (s, 1H), 9.61 (t, *J* = 4.4 Hz, 2H), 9.69 (d, *J* = 4.8 Hz, 2H), 9.75 (dd, *J*₁ = 4.8 Hz, *J*₂ = 6.8 Hz, 2H), 9.92 (t, *J* = 4.8 Hz, 2H), 10.53 (s, 1H).

Synthesis of compound **3**

To a solution of compound **2** (150 mg, 0.115 mmol) was added TBAF (0.15 mL of 1.0 M solution in THF, 0.15 mmol) in THF (5 mL). The solution was stirred under N₂ for 30 min to obtain intermediate, and then added mixture of compound **1** (150 mg, 0.124 mmol) in dry THF (10 mL) and triethylamine (5 mL). The solution was degassed with dinitrogen for 20 min; then Pd(PPh₃)₄ (11 mg, 0.01 mmol) and CuI (2 mg, 0.01 mmol) were added to the mixture. The reaction mixture was then stirred at 50°C for overnight under nitrogen. The solvent was removed in vacuo, and the residue was purified on a column chromatograph (silica gel) using CHCl₃ as eluent. Recrystallization from CHCl₃/CH₃OH gave compound **3** (165 mg, 63%). Compound **3** does not show satisfied NMR spectra due to its expanded π structure. (MALDI-TOF, *m/z*) calculated for C₁₄₄H₁₉₈N₈O₆Zn₂: 2267.4032; found: 2267.3987.

Synthesis of CS-DP

Compound **3** (150 mg, 0.066 mmol) was dissolved in a solution of dry CHCl₃, two drops of piperdine and then 3-ethylrhodanine (106 mg, 0.66 mmol) were added, and the resulting solution was refluxed and stirred for 12h under argon. The reaction was quenched into water (30 mL). The aqueous layers were extracted with CHCl₃ (3 × 20 mL). The organic layer was dried over NaSO₄. After removal of solvent, it was purified by chromatography on a silica gel column using CHCl₃ as eluant and was purified by preparative thin layer chromatography using a CHCl₃ as eluents. Then the crude solid was recrystallized from CHCl₃ and CH₃OH mixture to afford **CS-DP** as a

gray green solid (102 mg, 60%). **CS-DP** does not show satisfied NMR spectra due to its expanded π structure. (MALDI-TOF, m/z) calculated for $C_{154}H_{208}N_{10}O_6S_4Zn_2$: 2553.2846; found: 2553.3750.

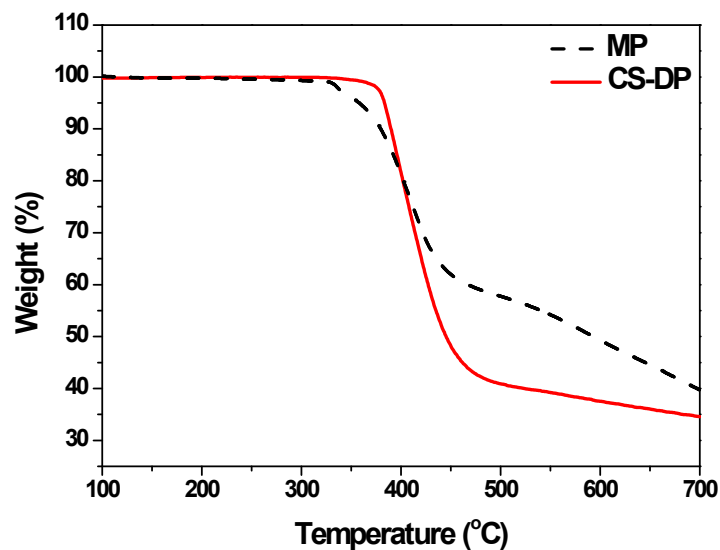


Figure S2. Thermogravimetric analysis of **MP** and **CS-DP**.

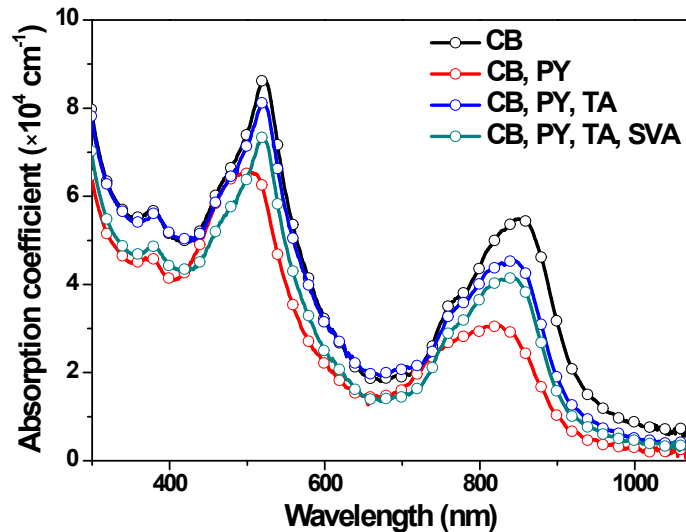


Figure S3. Absorption spectra of **CS-DP/PC₇₁BM** films under different processing conditions.

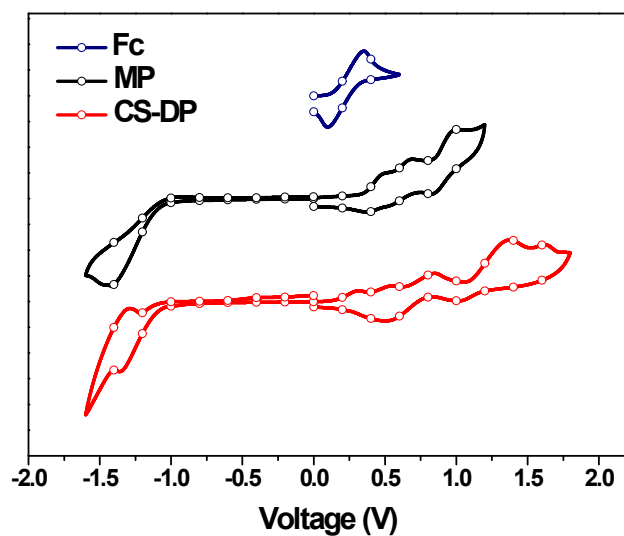


Figure S4. Cyclic voltammogram of MP and CS-DP measured in 0.1 mol L^{-1} TBAPF₆ CH₂Cl₂ solutions.

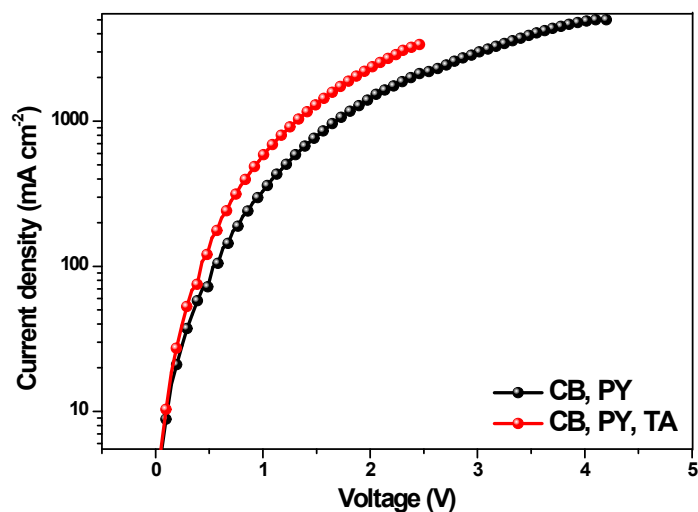


Figure S5. The space charge limited current (SCLC) curves of CS-DP with additive. The sample without and with TA treatment exhibit a high hole mobilities of $7.75 \times 10^{-5} \text{ cm}^2 \text{ V}^{-1} \text{ s}^{-1}$ and $1.40 \times 10^{-4} \text{ cm}^2 \text{ V}^{-1} \text{ s}^{-1}$, respectively.

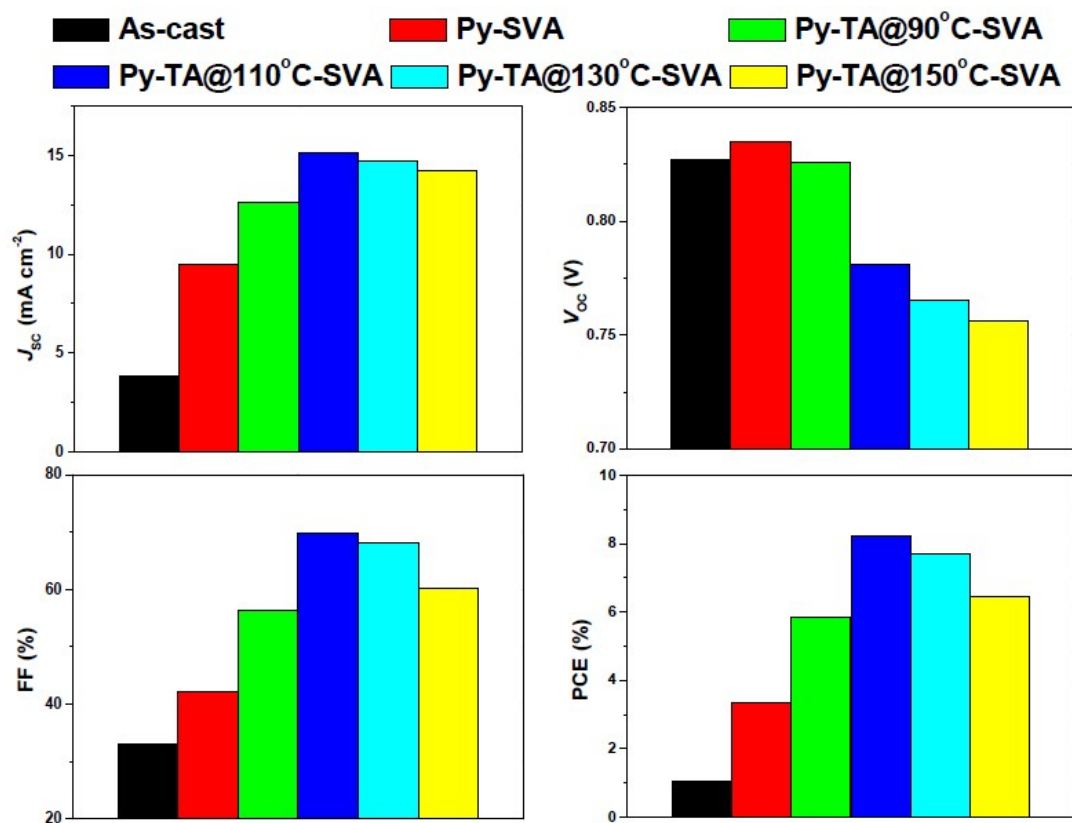


Figure S6. Plots of key parameters dependent on the device processing conditions.

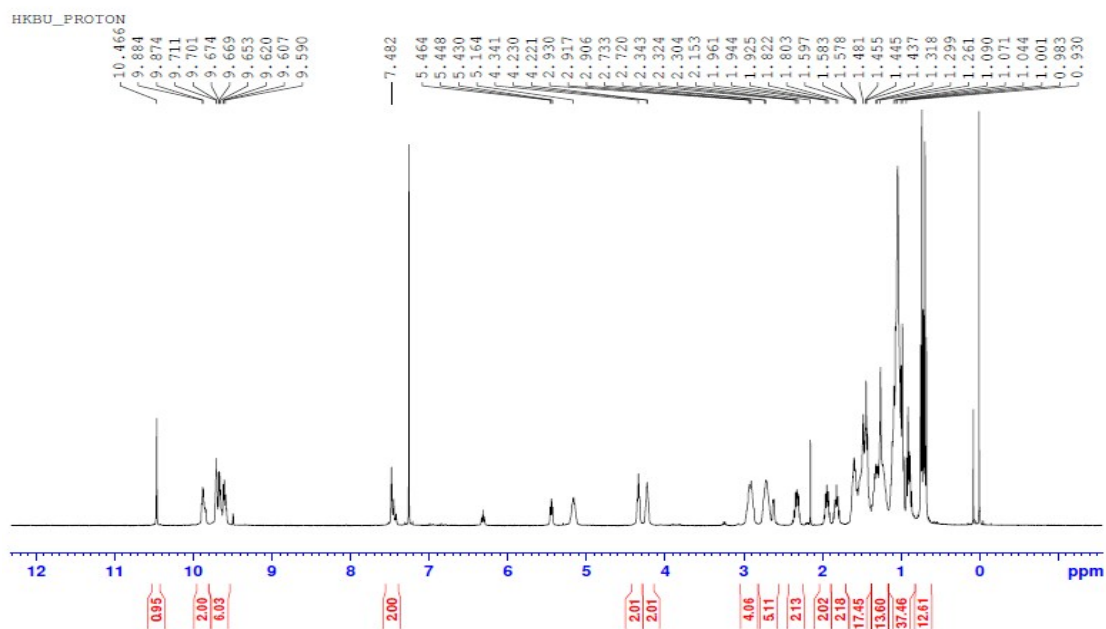


Figure S7. The ¹H NMR (400 MHz) spectrum of compound **1** in CDCl₃.

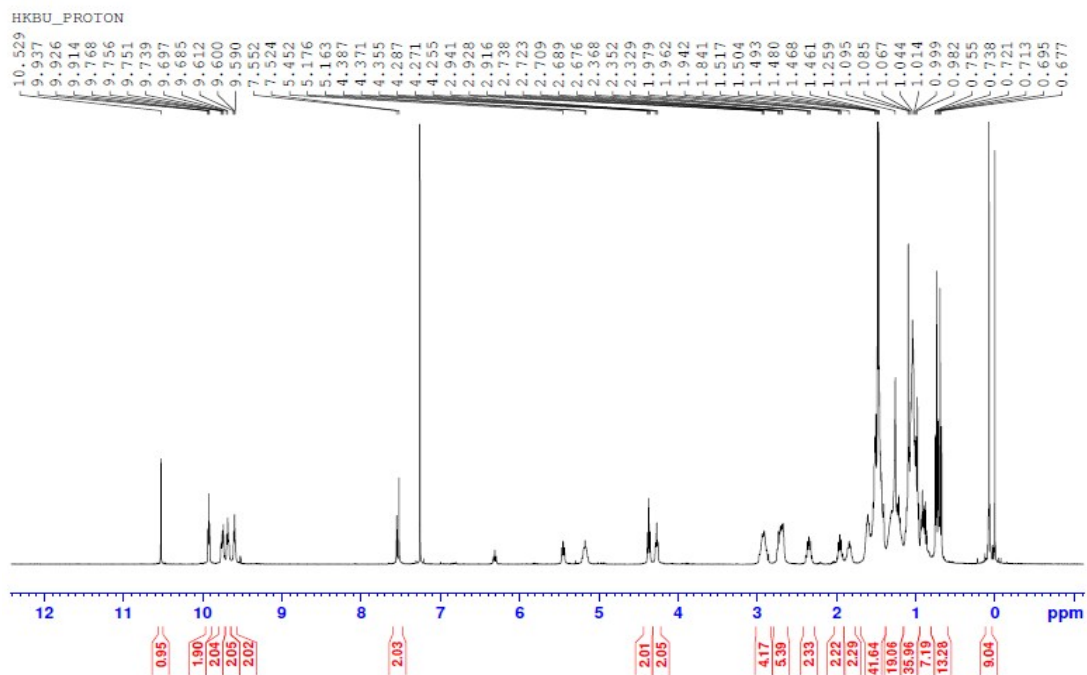


Figure S8. The ^1H NMR spectrum of compound **2** in CDCl_3 .

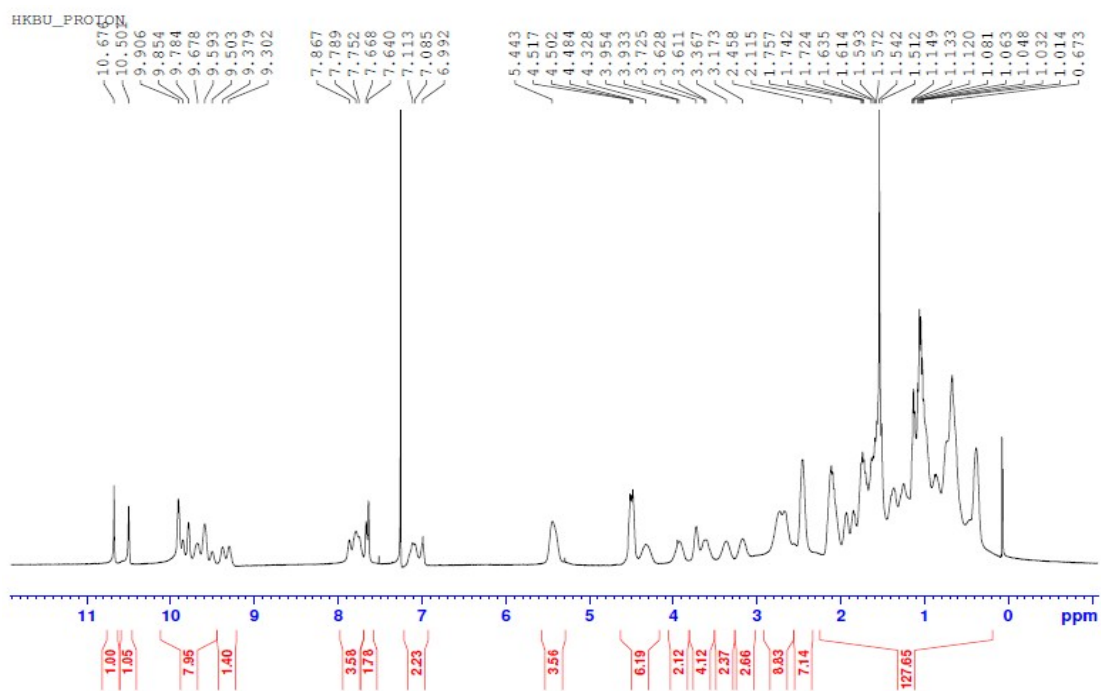


Figure S9. The ^1H NMR spectrum of **3** in CDCl_3 .

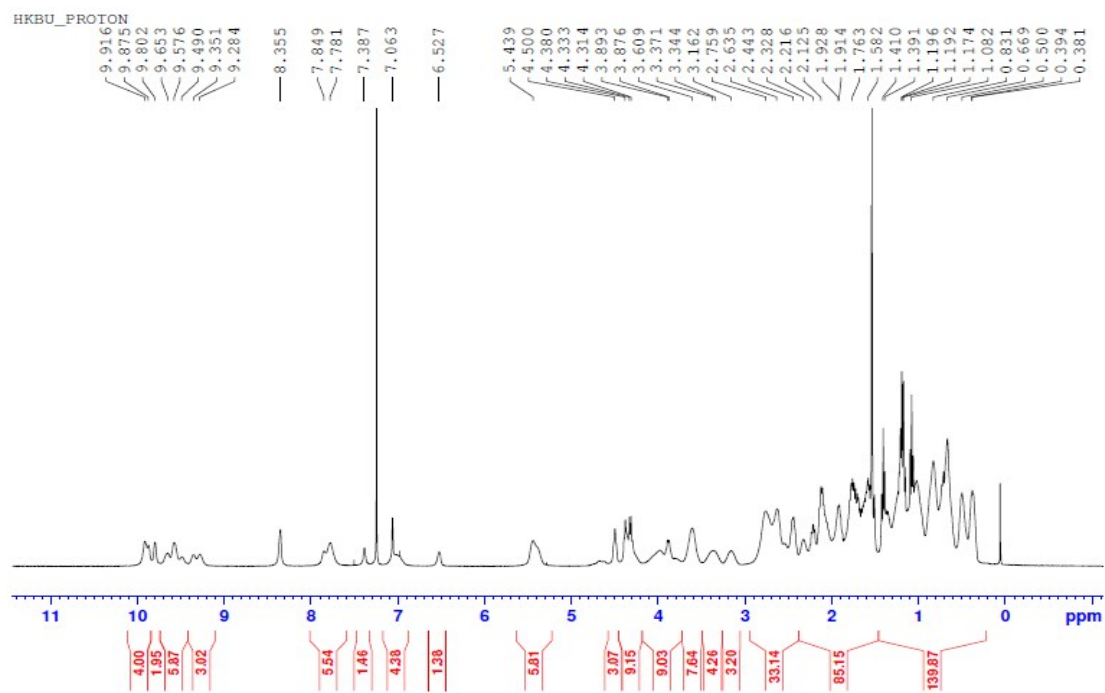


Figure S10. The ^1H NMR spectrum of CS-DP in CDCl_3 .

HONG KONG BAPTIST UNIVERSITY, DEPARTMENT OF CHEMISTRY (MALDI-TOF)

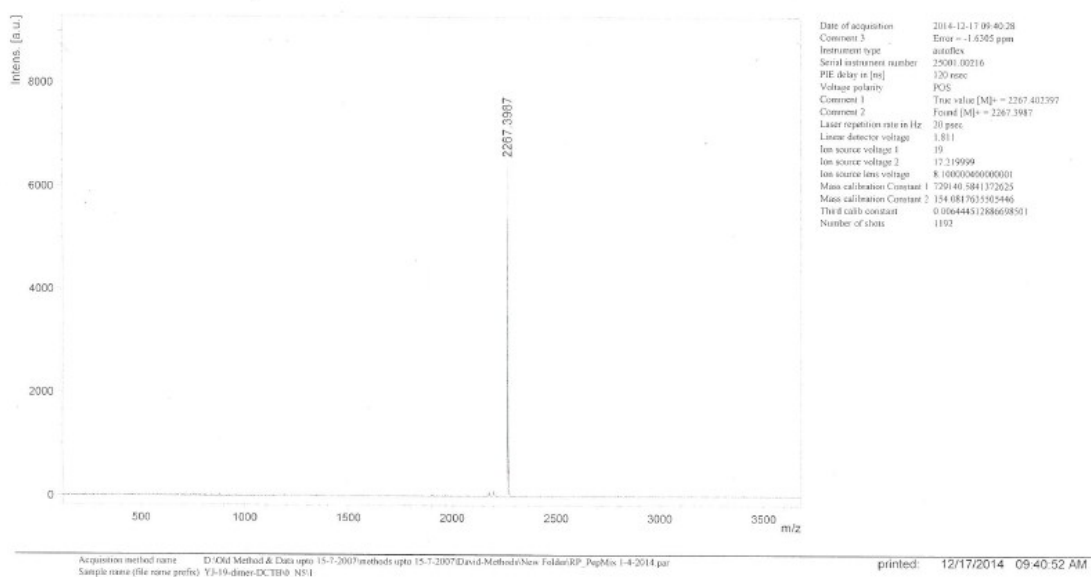


Figure S11. The MALDI-TOF mass spectrum of compound **3**.

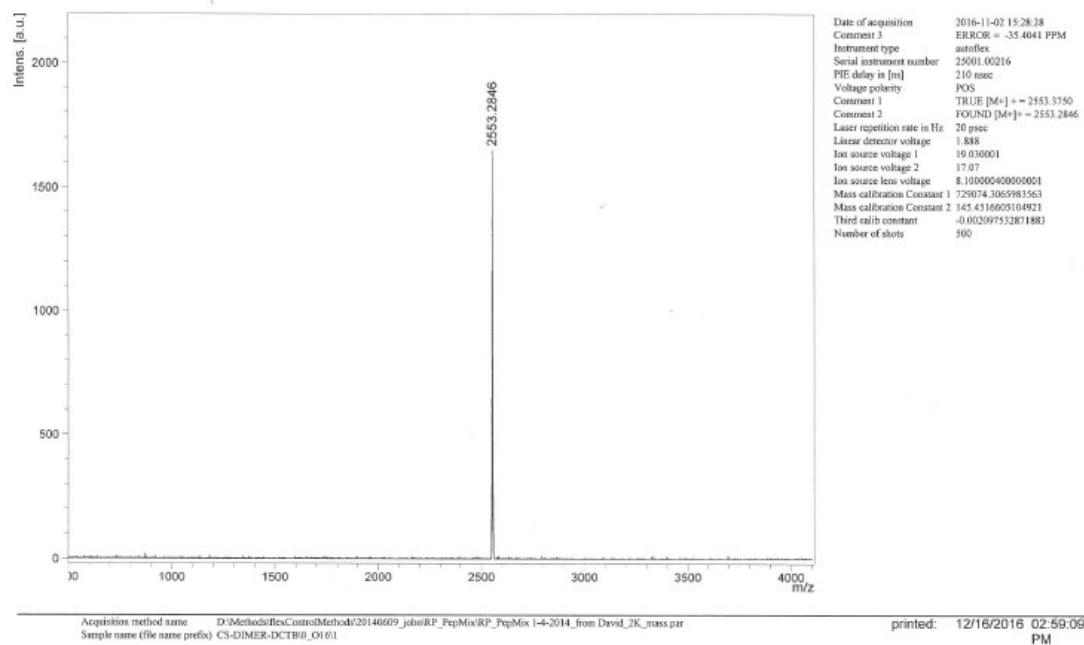


Figure S12. The MALDI-TOF mass spectrum of **CS-DP**.